that move slowly and are not highly excited (i.e., we assume $\partial/\partial\mathbf{R}$, $\partial/\partial\zeta$, and $\alpha\zeta$ are all of order $\alpha^{1/2}$). Equation (28) then describes a free particle and a set of uncoupled harmonic oscillators. For an eigenstate of $-i(\partial/\partial\mathbf{R})$ having eigenvalue $\mathbf{k}=\alpha^{-1}\boldsymbol{\kappa}$, and being in the ground state with respect to ζ, the energy is

$$E=+\alpha^2W_0+\frac{27\sqrt{\pi}}{32}\alpha^{-2}\kappa^2+\frac{\alpha}{2}\sum_{n>3}\sqrt{\gamma_n}.$$

Hence the polaron effective mass is given by

$$\frac{m(\text{polaron})}{m(\text{band})}=\frac{32}{27\sqrt{\pi}}\alpha^2.$$

We see that it is proportional to α^2 rather than α^4, as in the optical-polaron problem. The reason for this is clearly that the dynamical behavior of the acoustic phonons is different from that of optical phonons.

PHYSICAL REVIEW VOLUME 179, NUMBER 3 15 MARCH 1969

Calculation of Dynamical Surface Properties of Noble-Gas Crystals. I. The Quasiharmonic Approximation*

R. E. ALLEN AND F. W. DE WETTE
Department of Physics, University of Texas, Austin, Texas 78712
(Received 25 October 1968)

Various dynamical surface properties have been calculated for noble-gas crystals in the quasiharmonic approximation. The calculations were carried out for slab-shaped fcc crystals in which the atoms interact through a Lennard-Jones potential. Changes in the force constants near the surface caused by changes in the interplanar spacings (static displacements) have been taken into account. Mean-square amplitudes and mean-square velocities of vibration were calculated for the (100), (111), and (110) surfaces. The surface specific heat, which was calculated for the (100) surface, is found to be positive and to vary as T^2 at low temperatures. So-called *dynamic displacements*, which are the displacements of the mean atomic positions in a vibrating crystal with free surfaces from the mean positions in the bulk, were calculated for the (100) surface. They are found to increase rapidly with temperature, indicating that thermal expansion is considerably greater at the surface than in the bulk. Some qualitative features of the static displacements for the (100), (111), and (110) surfaces are pointed out and explained. It is shown that the dynamical matrix for a general slab-shaped crystal can be reduced to a real symmetric matrix of the same size; this fact greatly facilitates calculations based on such models. The fact that the mean-square amplitudes diverge at finite temperatures for infinite slab-shaped crystals is discussed; it is found that accurate calculations based on slab-shaped models are possible despite this feature.

I. INTRODUCTION

In recent years there has been considerable interest in the study of structural and dynamical properties of crystal surfaces through low-energy electron diffraction experiments. Measurements of the mean-square amplitudes[1] of vibration, for example, have been performed for nickel,[2] silver,[3] platinum,[4] and palladium and lead.[5] In parallel with the experiments there have been various theoretical studies and calculations. The work up to a few years ago has been summarized in a review article by Maradudin.[6] More recent work includes a general analytical treatment of the static displacements and vibrational modes in a semi-infinite crystal by Feuchtwang,[7] calculations of the mean-square amplitudes in a nearest-neighbor, central-force model by Wallis, Clark, and Herman,[8] and calculations of dynamical quantities for microcrystallites by Kothari and Singal.[9]

Qualitative agreement has been found between the experimental and theoretical results for the mean-square amplitudes of vibration.[10] However, a detailed comparison between theory and experiment has not been possible, since the experiments have been performed on metal surfaces while no first-principle calculation of dynamical surface effects in metals has been carried out to this date, because of the inherent difficulties in the theory of the lattice dynamics of

* Work supported by the U. S. Air Force Office of Scientific Research under Grant No. AF-AFOSR 1257-67.

[1] The quantities frequently called "mean-square displacements" we call "mean-square amplitudes," in order to avoid confusion with the displacements of the mean atomic positions. Definitions of "mean displacements" and "mean-square amplitudes" are given in Secs. I and III, respectively. There has already been some confusion between these two quantities, namely, in Ref. 5.

[2] A. U. Mac Rae, Surface Sci. 2, 522 (1964).

[3] E. R. Jones, J. T. McKinney, and M. B. Webb, Phys. Rev. 151, 476 (1966).

[4] H. B. Lyon and G. A. Somorjai, J. Chem. Phys. 44, 3707 (1966).

[5] R. M. Goodman, H. H. Farrell, and G. A. Somorjai, J. Chem. Phys. 48, 1046 (1968).

[6] A. A. Maradudin, Solid State Phys. 18, 1 (1966).

[7] T. E. Feuchtwang, Phys. Rev. 155, 715 (1967).

[8] R. F. Wallis, B. C. Clark, and R. Herman, Phys. Rev. 167, 652 (1968).

[9] L. S. Kothari and C. M. Singal, Phys. Rev. 168, 952 (1968).

[10] B. C. Clark, R. Herman, and R. F. Wallis, Phys. Rev. 139, A860 (1965).

metals. As a consequence, past calculations have involved simplifying assumptions such as restriction to nearest-neighbor[10] or nearest- and next-nearest-neighbor[11] interactions, use of force constants which are the same at the surface as in the bulk, and restriction to the high-temperature limit.

In order to carry out a first-principle calculation of surface properties, avoiding all such approximations, it is necessary to have an accurate knowledge of the atomic interactions. The only group of substances for which this requirement is nearly satisfied is that of the noble-gas solids. It is well-known that the Lennard-Jones (6,12) potential gives an adequate description of the pair-wise interaction in these solids (see Sec. VIII). Some of the advantages of using the LJ potential are the following: First, dimensionless quantities can be introduced which do not depend upon the mass or the potential constants, so that the calculation is free of empirical parameters; i.e., it is not necessary to perform a separate calculation for each substance or to repeat the calculation for improved values of the potential constants. Second, interactions with all neighbors can be readily taken into account. Third, changes in the force constants near the surface can be determined and taken into account. Finally, a direct comparison of calculations based on the LJ potential and experiments on the noble-gas solids may be possible in the future. Aside from this possibility, however, a detailed calculation of surface effects in a realistic model is in itself of considerable interest.

In this paper we are primarily concerned with calculation of the following quantities: The mean-square amplitudes and mean-square velocities of vibration, the surface specific heat, and the displacements of the mean positions of atoms near the surface from the mean positions that these atoms would have in the bulk of the crystal.

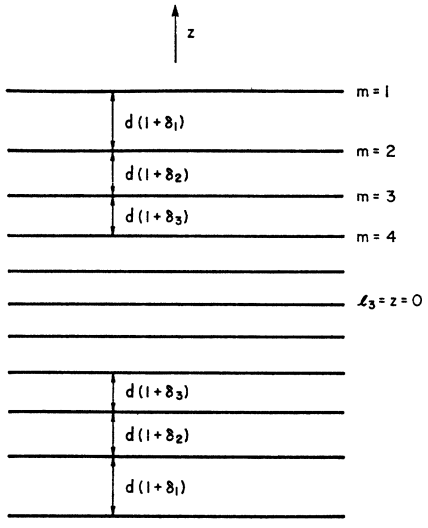

FIG. 1. Side view of slab-shaped crystal showing spacings between planes perpendicular to the z axis. d is the bulk interplanar spacing.

[11] A. A. Maradudin and J. Melngailis, Phys. Rev. 133, A1188 (1964).

The last set of quantities will be represented by δ_m, where m is an integer labeling the planes of the crystal which are parallel to the surface. This notation is clarified by Fig. 1, which shows a side-view of a slab-shaped crystal. We take m to be 1 for the upper surface, 2 for the plane just below the surface, and so on. δ_m is defined to be the fractional change in the distance between the mth and $(m+1)$th planes; i.e.,

$$\delta_m = \frac{z_m - z_{m+1}}{\text{interplanar spacing in bulk}} - 1, \qquad (1.1)$$

where z_m is the coordinate of the mth plane in the direction perpendicular to the surface.

In general, we shall refer to the δ_m as the *mean displacements*, or simply the *displacements*. If they are determined by minimizing the static energy, we shall call them the *static displacements*. If they are determined by minimizing the total free energy, including vibrational contributions, we shall call them the *dynamic displacements*. The static displacements, therefore, are displacements of the equilibrium positions in a static crystal. The dynamic displacements are displacements of the mean positions in a vibrating crystal.

In carrying out the dynamical calculations we have used the static rather than the dynamic displacements to determine the change in force constants near the surface. Our reason for doing so is that the static displacements are readily calculated and are independent of mass and potential constants, whereas the dynamic displacements are calculated with somewhat more difficulty and depend upon the de Boer parameter, which is different for each substance (see Sec. VI). If there is an appreciable difference in thermal expansion between the surface and the bulk, this approximation of using the static displacements should lead to errors in the calculated quantities at high temperatures. We shall find (in Sec. VI) that the thermal expansion is in fact considerably larger at the surface. However, we shall also see that at low temperatures it is a good approximation to use the static displacements.

In Sec. II we describe the general model and the method for calculating the static displacements. Two qualitative features of the static displacements, namely a "staircase" behavior for the (110) surface and a $1/m^3$ dependence for the deeper displacements, are explained in Appendix A. In Sec. III the procedure for dynamical calculations is outlined. Expressions for the dynamical matrix and physical quantities in the case of an LJ potential are given in Appendix B, and in Appendix C it is shown that the dynamical matrix for a slab-shaped crystal can, under very general conditions, be reduced to a real, symmetric matrix of the same size. Use of this reduced matrix results in a very

large reduction in the required computer time. The fact that the mean-square amplitudes diverge for an infinite slab-shaped crystal is discussed in Appendix D. In Sec. IV results are presented for the mean-square amplitudes and mean-square velocities; some qualitative features of these results are discussed. In Sec. V, tests of the accuracy of the method are described. Section VI deals with calculation of the dynamic displacements, and Sec. VII with the density of states and calculation of the surface specific heat. Finally, in Sec. VIII we give a general discussion of the work of this paper.

II. GENERAL MODEL AND STATIC DISPLACEMENTS

All the calculations of this paper were carried out for slab-shaped, face-centered cubic crystals, the two free surfaces of which are, respectively, (100), (111), and (110) planes of the crystal. It will be shown that the finite thickness of the model crystal does not have an important effect upon the results, provided that a sufficient number of planes of atoms are used. The atoms in the crystal are taken to interact through a Lennard-Jones (6,12) potential.

We denote by x and y two suitably chosen orthogonal directions in a plane parallel to the surface,[12] and by z the direction perpendicular to the surface. The number of planes in the model we call N_3, and the number of atoms per plane N. The planes are labeled by an integer m, the position of each plane is specified by l_3 (not necessarily an integer), and the position of an atom within a plane is specified by l_1 and l_2. It is convenient to choose the l_3 axis perpendicular to the surface (i.e., in the z direction), in which case the two-dimensional lattice represented by integer values of l_1 and l_2 is nonprimitive. The distance between the equilibrium positions of the atoms at $\mathbf{l}$ (l_1,l_2,l_3) and $\mathbf{l}'$ (l_1',l_2',l_3') is called $r_0^{ll'}$. We define a distance a such that the nearest-neighbor distance is equal to $\sqrt{2}a$.

In order to calculate the static displacements or the dynamical matrix it is necessary to carry out lattice summations which involve designating an atom in one plane as the origin and then summing over all the atoms in another (or the same) plane. These summations are performed most readily by summing over shells of atoms with the same distance from the origin. The convergence of such summations can be improved by special convergence techniques,[13] but in the present case relatively little computer time would be saved by such methods; we have used the direct summation method throughout.

In calculating the static displacements we assume that each plane is displaced as a whole in the direction perpendicular to the surface. One can easily see that such a displacement results in an equilibrium situation, and in II[14] we show that this equilibrium is stable for all three of the surfaces considered here. Our method of calculation is essentially that described by Alder, Vaisnys, and Jura.[15] The total static energy of the crystal is

$$\Phi=\tfrac{1}{2}N\sum_{l_3,l_3'}\sum_{l_1,l_2}4\epsilon\left[\left(\frac{\sigma}{r_0^{ll'}}\right)^{12}-\left(\frac{\sigma}{r_0^{ll'}}\right)^{6}\right], \quad (2.1)$$

where ϵ and σ are the familiar constants of the LJ potential. Φ is to be minimized with respect to the displacements δ_m; i.e., we have to satisfy the equations

$$\frac{\partial\Phi}{\partial\delta_m}=0, \quad m=1,2,\cdots. \quad (2.2)$$

The numerical procedure was to calculate δ_m using the previously determined $\delta_{m'}$ for $m'<m$ and to take $\delta_{m'}=0$ for $m'>m$ in the first iteration. Two complete iterations were used for the (100) and (111) surfaces and four for the (110) surface, which presents special problems (see below).

Calculations of the static displacements in semi-infinite crystals with an LJ potential have previously been carried out by Shuttleworth,[16] by Alder *et al.*, and by Benson and Claxton.[17] Only the first five displacements were determined, with the deeper ones taken to be zero. We have calculated all the displacements in models ranging from 11 to 51 planes in thickness, and our results for the (110) surface are slightly more accurate than those of Benson and Claxton. We find that the finite thickness of the crystal has only a very small effect on the results for $N_3\gtrsim 30$.

The results for the static displacements are shown in Fig. 2. Notice the unusual "staircase" behavior for the (110) surface; the rate of decrease with distance from the surface is alternately large and small. This behavior is due to the close spacing of the (110) planes: In the (100) and (111) cases, all the nearest neighbors for a given atom are in the same plane or adjacent planes. In the (110) case, however, there are nearest neighbors in the next planes also, so that each displacement is dependent upon those adjacent to it (see Appendix A). This coupling of the displacements requires that extra iterations be used in the calculation for the (110) surface. It should also be noted that the displacements decrease monotonically. (That they fail to do so in the results of Benson and Claxton is a

[12] The structures of the various surfaces and our choice for the x and y directions are shown in Fig. 1 of II. In particular, for the (110) surface the x and y axes are taken to point in the [1$\bar{1}$0] and [001] directions, respectively.

[13] B. M. E. van der Hoff and G. C. Benson, Can. J. Phys. **31**, 1087 (1953).

[14] R. E. Allen, F. W. de Wette, and A. Rahman, following paper, Phys. Rev. **179**, 887 (1969). We refer to this paper as II.

[15] B. J. Alder, J. R. Vaisnys, and G. Jura, J. Phys. Chem. Solids **11**, 182 (1959).

[16] R. Shuttleworth, Proc. Phys. Soc. (London) **A62**, 167 (1949).

[17] G. C. Benson and T. A. Claxton, J. Phys. Chem. Solids **25**, 367 (1964).

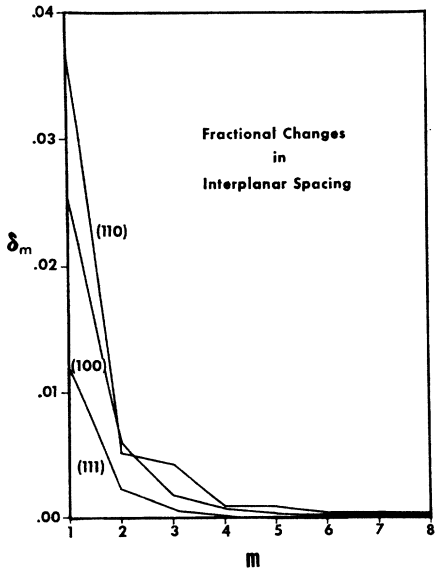

FIG. 2. Static displacements δ_m for (100), (111), and (110) surfaces expressed as fractional changes in the interplanar spacings.

peculiarity induced by the assumption that all displacements beyond the fifth are zero.)

We find that the displacements for all three surfaces fall off approximately as the inverse cube of the distance from the surface. This rule becomes increasingly better as the depth of the displacement increases, but is rather good for all displacements except the first in the (100) and (111) cases. In the (110) case the "staircase" behavior is superimposed upon the $1/m^3$ behavior until $m \geq 8$. Our results are thus in accord with the demonstration of Alder *et al.* that the deeper displacements should decrease as $1/m^3$ for the (100) surface and imply that this rule is of more general validity. In Appendix B we show that in fact the following is true: If the particles in a semi-infinite crystal interact through a potential $\phi(\mathbf{r})$ such that for large $|\mathbf{r}|$

$$\phi(\mathbf{r}) \propto \frac{1}{|\mathbf{r}|^p}, \tag{2.3}$$

where p is an integer greater than 3, then for large m

$$\delta_m \propto \frac{1}{m^{p-3}}. \tag{2.4}$$

For any potential in which a van der Waals part dominates at large distances $p=6$, and as a result the inverse cube behavior holds.

III. PROCEDURE FOR DYNAMICAL CALCULATIONS

In the previous section we were concerned with surface effects in a static crystal. In this section we consider the surface properties of a crystal in which the atoms are vibrating. In order to make the dynamical problem amenable to calculations, we need to assume, first, that the crystal has a finite thickness and, second, that the vibrations obey the usual periodic boundary conditions with respect to translations parallel to the surface. This model has been previously used by Clark, Herman, and Wallis[10] and has been discussed by Maradudin.[6] The justification for the model is that the correct results for a semi-infinite crystal are obtained as the periodicity length and the thickness simultaneously approach infinity (see Sec. V and Appendix D).

Let $u_\alpha(\mathbf{l})$ be the α component ($\alpha = x, y, z$) of the displacement of the $\mathbf{l}$th atom from its mean position. The coordinates of the mean position we call x_0^l, y_0^l, and z_0^l. Because of the two-dimensional periodic boundary conditions, the normal mode solutions have the form

$$u_\alpha(\mathbf{l}) = M^{-1/2}\xi_\alpha(l_3)e^{i\omega t}e^{-i(q_x x_0^l + q_y y_0^l)}, \tag{3.1}$$

where M is the atomic mass and ω is the vibrational frequency. The quantities $\xi_\alpha(l_3)$ will turn out to be components of the eigenvectors of the dynamical matrix. The allowed values of q_x and q_y are determined by the periodic boundary conditions; they may be taken to lie in the first two-dimensional Brillouin zone for the primitive lattice associated with a plane of atoms parallel to the surface (see Fig. 3).

Henceforth we shall write two-dimensional vectors without boldface, so that $q=(q_x,q_y)$, $l=(l_1,l_2)$, and $r_0^l=(x_0^l,y_0^l)$, whereas $\mathbf{r}_0^l=(x_0^l,y_0^l,z_0^l)$. In this notation, $q\cdot r_0^l = q_x x_0^l + q_y y_0^l$.

When Eq. (3.1) is substituted into the equation of motion in the quasiharmonic approximation, one obtains the usual eigenvalue equation

$$\sum_{l_3',\beta} D_{\alpha\beta}(l_3 l_3')\xi_\beta(l_3';p) = \omega_p^2 \xi_\alpha(l_3;p), \tag{3.2}$$

where $p=1, 2, \cdots, 3N_3$ labels the branches of ω for a given q. The dynamical matrix $D_{\alpha\beta}(l_3 l_3')$ is defined by

$$D_{\alpha\beta}(l_3 l_3') = \frac{1}{M}\sum_{l'} \Phi_{\alpha\beta}(\mathbf{l}\mathbf{l}') \exp[iq\cdot(r_0^l - r_0^{l'})], \tag{3.3}$$

with

$$\Phi_{\alpha\beta}(\mathbf{l}\mathbf{l}') = \left(\frac{\partial^2\Phi}{\partial u_\alpha(\mathbf{l})\partial u_\beta(\mathbf{l}')}\right)_0. \tag{3.4}$$

The subscript "0" in Eq. (3.4) indicates that the force constants $\Phi_{\alpha\beta}(\mathbf{l}\mathbf{l}')$ are to be evaluated at the true mean positions of the atoms, with the displacements from the bulk positions taken into account.

The general solution for $u_\alpha(\mathbf{l})$ is a superposition of the normal mode solutions of Eq. (3.1)

$$u_\alpha(\mathbf{l}) = N^{-1/2}M^{-1/2}\sum_{q,p} Q(qp)\xi_\alpha(l_3;qp)e^{-iq\cdot r_0 l}. \tag{3.5}$$

Using this solution, one can obtain an expression for the mean-square amplitude $\langle u_\alpha^2(l_3)\rangle$, which is defined

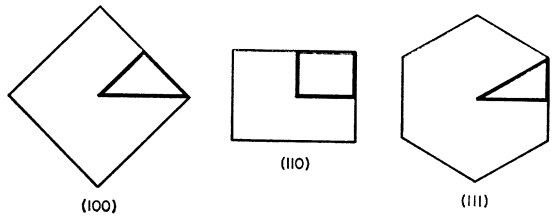

FIG. 3. Two-dimensional Brillouin zones associated with (100), (111), and (110) surfaces for fcc lattices.

as the thermal average of $u_\alpha^2(\mathbf{l})$, in terms of the eigenvalues ω^2 and eigenvectors $\xi_\alpha(l_3)$ of the dynamical matrix. (See pp. 236–237 of Ref. 18 for the derivation.) The result is

$$\langle u_\alpha^2(l_3)\rangle=\frac{\hbar}{2NM}\sum_{q,p}{}'|\,\xi_\alpha(l_3;\,qp)\,|^2 \times\frac{\coth[\hbar\omega_p(q)/2k_BT]}{\omega_p(q)}, \quad (3.6)$$

where k_B is the Boltzmann constant and T is the temperature. Similarly, if $\mathbf{p}(\mathbf{l})$ is the momentum of the particle labeled by $\mathbf{l}$, the mean-square momentum $\langle p_\alpha^2(l_3)\rangle$ is given by

$$\langle p_\alpha^2(l_3)\rangle=\frac{\hbar M}{2N}\sum_{q,p}{}'|\,\xi_\alpha(l_3;\,qp)\,|^2 \times\omega_p(q)\coth[\hbar\omega_p(q)/2k_BT]. \quad (3.7)$$

The Helmholtz free energy F and the specific heat at constant volume C_v can be expressed in terms of the frequencies alone

$$F=k_BT\sum_{q,p}{}'\ln\left\{2\sinh\left(\frac{\hbar\omega_p(q)}{2k_BT}\right)\right\}, \quad (3.8)$$

and

$$C_v=k_B\sum_{q,p}{}'\left(\frac{\hbar\omega_p(q)}{2k_BT}\right)^2\Big/\sinh^2\left(\frac{\hbar\omega_p(q)}{2k_BT}\right) \quad (3.9)$$

(see pp. 45–46 of Ref. 18).

Calculations of the above dynamical quantities based on Eqs. (3.6)–(3.9) are straightforward, but two facts should be mentioned: First, the point $q_x=q_y=0$ is to be included in the summations, but the three $\omega=0$ modes are not to be included (as indicated by the primes on the summations) because these modes correspond to uniform translations of the crystal. Second, the expression for the mean-square amplitude diverges at nonzero temperatures[19] (see Appendix D). The divergence is very slow, so that the root-mean-square amplitude is of the order of a lattice spacing only for crystals much larger than the solar system. However, because the divergence is logarithmic and the mean-square amplitudes are small, the effect of the divergence can be observed even for small periodicity lengths. The mean-square amplitudes can be calculated with reasonable accuracy despite this fact (see Appendix D), but it does not make sense to speak of calculating the mean-square amplitudes for a slab-shaped crystal of infinite extent. Properly, one calculates these quantities for a crystal whose periodicity length and thickness are approximately equal and are large enough so that their finite values have only a small effect on the results.

[18] A. A. Maradudin, E. W. Montroll, and G. H. Weiss, *Theory of Lattice Dynamics in the Harmonic Approximation* (Academic Press Inc., New York, 1963).

[19] We wish to thank Dr. B. J. Alder for drawing our attention to this fact.

IV. MEAN-SQUARE AMPLITUDES AND MEAN-SQUARE VELOCITIES

Using the procedure outlined in Sec. III, we have calculated the mean-square amplitudes and mean-square velocities of vibration for the (100), (111), and (110) surfaces at various temperatures and densities. Some typical results are given in Figs. 4–10 and in Table I. All these results were obtained with a crystal 21 layers in thickness. For the (100) and (111) surfaces, 30 q points were used in the irreducible element of the two-dimensional Brillouin zone, yielding 1890 (30×3×21) independent frequencies; 36 q points in the irreducible element were used for the (110) surface.

It is a well-established fact that $\langle u^2\rangle$ increases and $\langle p^2\rangle$ decreases toward the surface, because surface atoms are less tightly bound than those in the bulk, and that near the surface these quantities are not isotropic even in cubic crystals; e.g., $\langle u_z^2\rangle\neq\langle u_x^2\rangle$. The qualitative features of the temperature dependence of $\langle u^2\rangle$ and $\langle p^2\rangle$ for constant density follow from Eqs. (3.6) and (3.7). At very low temperatures $\langle u^2\rangle$ and $\langle p^2\rangle$ are approximately constant. At high temperatures $\langle u^2\rangle$ and $\langle p^2\rangle$ are proportional to T, and $\langle p^2\rangle$ is the same at the surface as in the bulk of the crystal. When the temperature-dependence of the density and the dynamic displacements are taken into account, the high-tem-

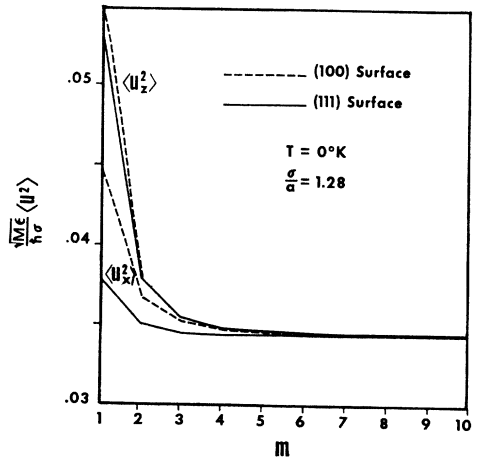

FIG. 4. Mean-square amplitudes $\langle u_x^2\rangle$ and $\langle u_z^2\rangle$ for (100) and (111) surfaces at $T=0$°K and $\sigma/a=1.28$.

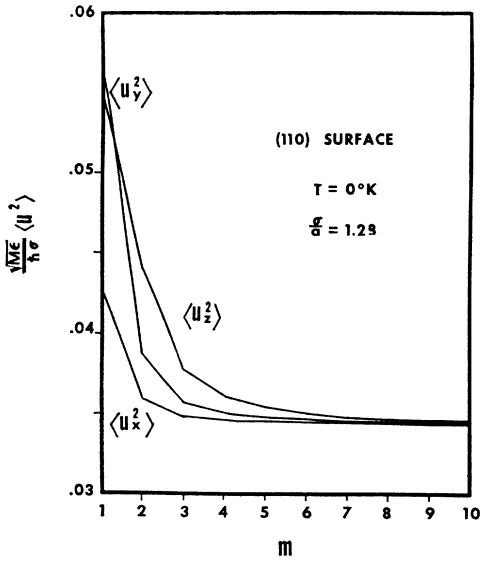

FIG. 5. Mean-square amplitudes $\langle u_x^2\rangle$, $\langle u_y^2\rangle$, and $\langle u_z^2\rangle$ for (110) surface at $T=0°K$ and $\sigma/a=1.28$.

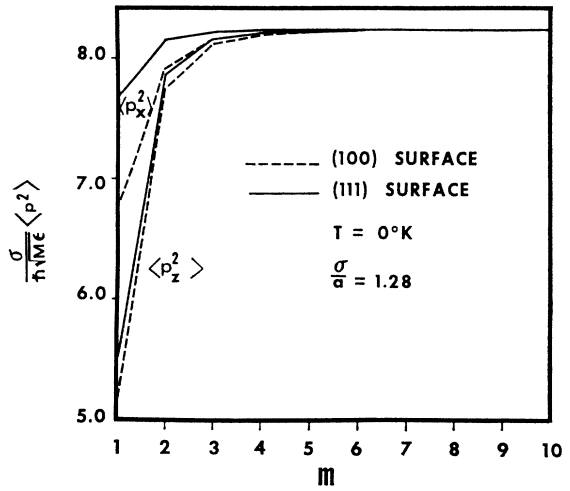

FIG. 6. Mean-square momenta $\langle p_x^2\rangle$ and $\langle p_z^2\rangle$ for (100) and (111) surfaces at $T=0°K$ and $\sigma/a=1.28$.

perature behavior is not so simple. The results of Table I, Fig. 11, and Fig. 12 show, respectively, that $\langle u^2\rangle$ increases as the density decreases, that the dynamic displacements increase with temperature, and that the mean-square amplitudes at the surface increase with the dynamic displacements. Consequently, the mean-square amplitudes will actually increase faster than linearly as the temperature increases.

One qualitative feature which is not shown in the figures, but which can be seen in Table II, is that the ratio $\langle u^2\rangle_{\text{surface}}/\langle u^2\rangle_{\text{bulk}}$ undergoes a pronounced increase in passing from $T=0°K$ to the high-temperature regime. This feature can be explained as follows: At absolute zero, the expression for $\langle u^2(l_3)\rangle$ in Eq. (3.6) involves summing $|\xi_\alpha(l_3)|^2/\omega$ over all modes; the expression for $\langle p^2(l_3)\rangle$ in Eq. (3.7) involves summing $|\xi_\alpha(l_3)|^2\omega$. Since $\langle u^2(l_3)\rangle$ increases as the surface is approached (i.e., as l_3 increases) and $\langle p^2(l_3)\rangle$ decreases, $|\xi_\alpha(l_3)|^2$ must on the average increase for small ω as the surface is approached and must decrease for large ω. At $T=0°K$, the summand in Eq. (3.6) is proportional to $1/\omega$, and for high T it is proportional to $1/\omega^2$. Consequently, the lower frequencies, which serve to increase $\langle u^2\rangle_{\text{surface}}$ with respect to $\langle u^2\rangle_{\text{bulk}}$, are more important at high temperatures, and as the temperature increases $\langle u^2\rangle_{\text{surface}}$ gains with respect to $\langle u^2\rangle_{\text{bulk}}$.

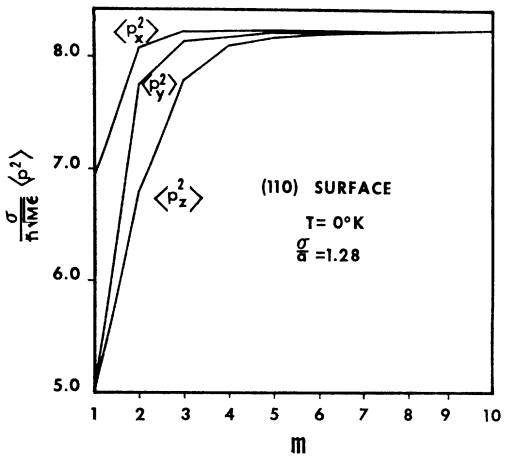

FIG. 7. Mean-square momenta $\langle p_x^2\rangle$, $\langle p_y^2\rangle$, and $\langle p_z^2\rangle$ for (110) surface at $T=0°K$ and $\sigma/a=1.28$.

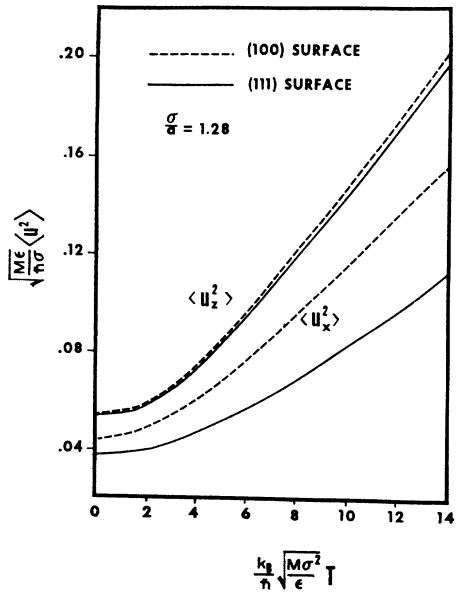

FIG. 8. Temperature dependence of mean-square amplitudes $\langle u_x^2\rangle$ and $\langle u_z^2\rangle$ for (100) and (111) surfaces at $\sigma/a=1.28$.

V. TESTS OF THE MODEL AND EFFECT OF SIMPLIFYING ASSUMPTIONS

One important question which has to be considered is the effect of the finite thickness of the crystal on the calculated quantities. In order to test this effect, we

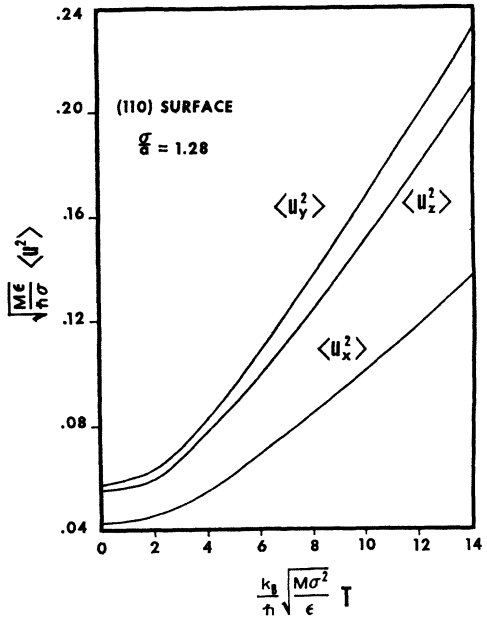

FIG. 9. Temperature dependence of mean-square amplitudes $\langle u_z^2\rangle$, $\langle u_y^2\rangle$, and $\langle u_x^2\rangle$ for (110) surface at $\sigma/a=1.28$.

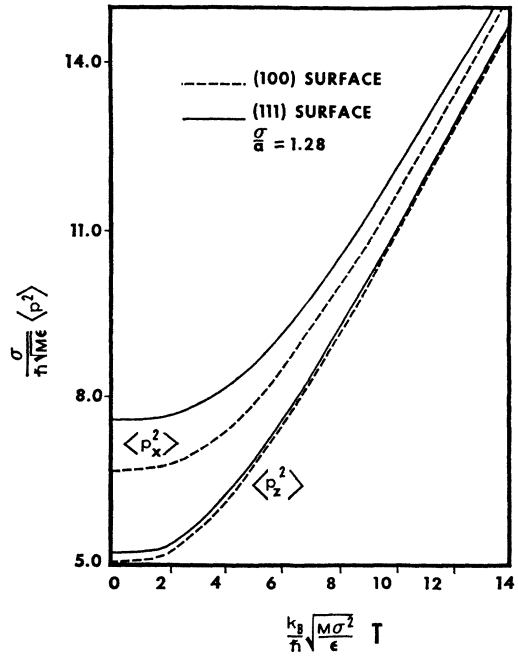

FIG. 10. Temperature dependence of mean-square momenta $\langle p_z^2\rangle$ and $\langle p_x^2\rangle$ for (100) and (111) surfaces at $\sigma/a=1.28$.

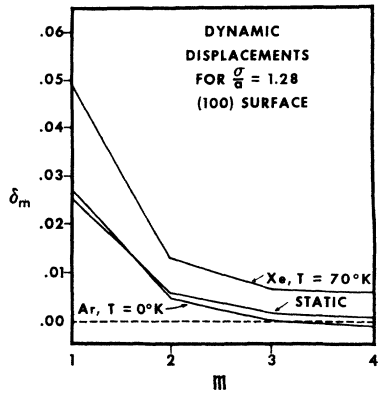

FIG. 11. Static displacements δ_m for (100) surface compared with dynamic displacements for Ar at 0°K and for Xe at 70°K.

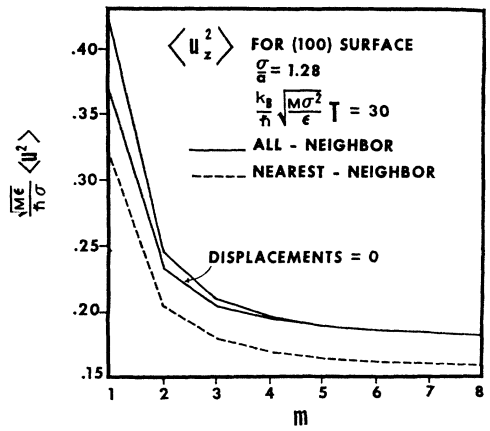

FIG. 12. Mean-square amplitudes $\langle u_z^2\rangle$ normal to the (100) surface at $\sigma/a=1.28$ for all-neighbor interaction with static displacements taken into account, all-neighbor interaction neglecting static displacements, and nearest-neighbor interaction neglecting static displacements, for a temperature slightly above the Debye temperature.

TABLE I. Dimensionless mean-square amplitudes $(M\epsilon)^{1/2}\langle u^2\rangle/\hbar\sigma$ at the surface for $T=0$°K and densities given by $\sigma/a=1.30$, 1.28, 1.26, and 1.24.

Surface	Component	1.30	1.28	1.26	1.24
(100)	$\langle u_x^2\rangle$	0.0389	0.0447	0.0519	0.0607
	$\langle u_z^2\rangle$	0.0480	0.0547	0.0627	0.0725
(111)	$\langle u_x^2\rangle$	0.0330	0.0379	0.0440	0.0515
	$\langle u_z^2\rangle$	0.0474	0.0537	0.0612	0.0702
(110)	$\langle u_x^2\rangle$	0.0371	0.0427	0.0495	0.0581
	$\langle u_y^2\rangle$	0.0504	0.0577	0.0667	0.0778
	$\langle u_z^2\rangle$	0.0484	0.0555	0.0641	0.0747
bulk	$\langle u^2\rangle$	0.0300	0.0344	0.0398	0.0464

performed calculations for models 11, 21, and 31 layers in thickness, for both the (100) and (110) surfaces. In addition, we carried out an independent calculation for the bulk. Table II contains the mean-square amplitudes for the bulk, and for the surface and the center plane of each of the three models with a (100) surface.

TABLE II. Effect of thickness and denseness of sample points on dimensionless mean-square amplitudes $(M\epsilon)^{1/2}\langle u^2\rangle/\hbar\sigma$ for (100) surface at $\sigma/a=1.28$.

$\frac{k_B}{\hbar}\left(\frac{M\sigma^2}{\epsilon}\right)^{1/2}T$	Number of layers	Number of points in irreducible element	$\langle u_z^2\rangle$ at surface	$\langle u_z^2\rangle$ at center	$\langle u^2\rangle$ in bulk
0	11	30	0.05474	0.03466	0.03437
	21	30	0.05468	0.03437	
	31	30	0.05468	0.03435	
	21	9	0.05472	0.03442	
	21	64	0.05449	0.03426	
70	11	30	0.9916	0.4603	0.4218
	21	30	0.9785	0.4166	
	31	30	0.9784	0.4130	
	21	9	0.9464	0.3984	
	21	64	0.9906	0.4316	

It can be seen that the effect of the finite thickness (and of the number of sample points in the Brillouin zone) is somewhat greater in the high-temperature regime than at absolute zero. This fact is related to the divergence of the mean-square amplitudes at high temperatures in an infinite slab-shaped crystal (see Appendix D and Ref. 25).

Another test was carried out to determine the effect of varying the number of sample points used in the irreducible element of the two-dimensional Brillouin zone. The results of calculations for the (100) surface with 9, 30, and 64 sample points are given in Table II. The results differ by only a few percent even in the high-temperature regime. An independent test is again provided by the bulk calculation, which was performed with a much finer mesh (10569 points in 1/48th of the three-dimensional Brillouin zone). It can be seen that the results for the center layer all agree with those for the bulk to within a few percent.

It is interesting to investigate the effect that the simplifying assumptions used by other workers have on the present results, since this effect provides a direct measure of the error introduced by these assumptions (in the case of an LJ potential). Clark, Herman, and Wallis[10] assumed a nearest-neighbor force law of the form

$$F_\alpha^{ll'}=k\sum_\beta \frac{\alpha_0^{ll'}\beta_0^{ll'}}{(r_0^{ll'})^2}[u_\beta(\mathbf{l})-u_\beta(\mathbf{l}')], \qquad (5.1)$$

where k is a constant. Here $\alpha_0^{ll'}$ is the α component of the vector $(\mathbf{r}_0^l-\mathbf{r}_0^{l'})$, where $\alpha=x$, y, or z. The force law for an LJ potential in the quasiharmonic approximation can be put in the form (5.1) by setting all displacements equal to zero, discarding forces due to atoms which are not nearest neighbors, and discarding a term in the nearest-neighbor force which is small. The results of a calculation of the mean-square amplitudes for such a nearest-neighbor interaction are shown in Fig. 12 together with the results for the all-neighbor interaction. Another calculation, the results of which are also graphed in Fig. 12, was carried out with an all-neighbor interaction, but with the displacements set equal to zero (i.e., no change in force constants at the surface). It is evident from the results that neglecting the change in force constants introduces substantial error into the calculated quantities at the surface.

Our calculated mean-square amplitudes for a nearest-neighbor interaction in the high-temperature limit are in agreement with those of Clark *et al.*, which were found by a slightly different method involving calculation of the inverse to the dynamical matrix rather than its eigensystem. These authors also tested the effect of thickness in their model and found it to be small.

It should be mentioned that effects of changes in the force constants at the surface have been considered in the literature. Vail[20] has evaluated the force constant changes in the case of a Morse potential and estimated their effect on the Debye-Waller factor. However, only one layer was allowed to relax in his model, and as a consequence the effect of the relaxation (i.e., the first static displacement) on the force constants and the Debye-Waller factor was underestimated. Wallis, Clark, and Herman[8] investigated the effect of force constant changes on the mean-square amplitudes in a nearest-neighbor model; they found that appropriate changes in the force constants lead to improved agreement with the experimental results for nickel.[2]

VI. DYNAMIC DISPLACEMENTS

In Sec. II we discussed the static displacements of the surface layers of a crystal. These displacements result from the asymmetry in the forces acting upon a surface atom. There is, however, an additional asymmetry at the surface of a *vibrating* crystal which affects the displacements of the mean positions: Consider a surface atom that is vibrating normal to the surface. Upon moving inward (i.e., toward the crystal), it is repelled by the atoms in the second layer, which cause it to reverse its direction of motion. When moving outward, however, it does not collide with any other atoms, but is forced to reverse its direction of motion by the *attraction* of the atoms in the crystal. Because of the asymmetry of the repulsive and attractive forces, this situation results in an additional outward shift of the mean position of the atom. It is obvious that these additional displacements will be strongly temperature-dependent. In fact, we find that at absolute zero they are small with respect to the static displacements, but at high temperatures they are of equal importance. As far as we know, these additional displacements have not been previously considered. The total displacements—i.e., the sum of the displacements resulting from static and dynamic causes—we call the *dynamic displacements*.

The calculation of the dynamic displacements is quite analogous to the calculation of the thermal expansion of bulk crystals; the mean lattice positions at

[20] J. Vail, Can. J. Phys. 45, 2661 (1967).

a given temperature are obtained by minimizing the Helmholtz free energy at that temperature with respect to the lattice positions. Since we assume that all atoms in a plane parallel to the surface are affected in the same way, we actually minimize the free energy with respect to the lattice spacings in the z direction. (To obtain the lattice spacings as a function of temperature, this process would have to be repeated for all temperatures.)

The total Helmholtz free energy is $\Phi+F$, where the static energy Φ is given by Eq. (2.1) and the vibrational free energy F is given by Eq. (3.8). If we define the dimensionless quantity Λ (the de Boer parameter) by

$$\Lambda=\hbar/(M\epsilon)^{1/2}\sigma \tag{6.1}$$

then the dimensionless free energy

$$\left(\frac{1}{\epsilon}\right)\Phi+\Lambda\left[\frac{1}{\hbar}\left(\frac{M\sigma^2}{\epsilon}\right)^{1/2}F\right] \tag{6.2}$$

is to be minimized with respect to the δ_m. Notice that Λ depends on the mass and potential constants, so that the dynamic displacements, unlike the static displacements, depend upon the atomic parameters and have to be recalculated for each substance.

The calculations reported here were carried out for the (100) surface with $\sigma/a=1.28$. In order to make the calculations feasible, only one displacement was allowed to vary at a time, while the others were assumed to have their static values; this approximation should be a good one because the displacements for the (100) surface depend only weakly upon one another. A calculation of the free energy was performed for five values of each of the first two displacements and for three values of the next two. The minimum of the expression (6.2) was then determined by an interpolation procedure. In addition to the values of Λ for the noble gases (taken from Horton and Leech[21]), an extra, very small value was chosen for a comparison with the results of molecular dynamics.[14]

Figure 11 shows some of the results.[22] Since the de Boer parameters of Ar, Kr, and Xe are rather small, one expects the static displacements to be a rather good approximation to the dynamic displacements at absolute zero for these substances. This expectation is confirmed by the results for Ar at 0°K. (Ar has the largest de Boer parameter of the three substances.) However, the dynamic displacements for Xe at 70°K are about double the static displacements. The dynamic displacements, therefore, undergo a rapid increase with temperature. According to the results of Sec. V, this fact implies that our approximation of setting the displacements equal to their static values will introduce large errors into the calculated mean-square amplitudes at high temperatures. The results for Ar at 0°K, however, show that at low temperatures such errors will be small.

Since we have defined both static and dynamic displacements as fractional changes in the interplanar spacing with respect to the bulk spacing at the same density, the fact that the dynamic displacements increase rapidly with temperature means that thermal expansion is much greater at the surface than in the bulk of the crystal.

VII. DENSITY OF STATES AND SURFACE SPECIFIC HEAT

Surface atoms may be thought of as less tightly bound than those in the bulk, since at the surface some interactions are missing and others are weakened by the displacements. Accordingly, one expects a downward shift in some of the vibrational frequencies of the crystal when there is a surface present. This shift should show up on a comparison of the density of states curves for the bulk and for a crystal with surface. We have calculated the density of states for a slab with (100) surfaces and a thickness of 21 layers, and have performed an independent calculation for the bulk. The results, given in Fig. 13, show that the expected downward shift in the frequencies of the slab-shaped crystals is indeed present. (The second graph is somewhat smoother than the first because more frequencies were determined in the bulk calculation than in the surface calculation.)

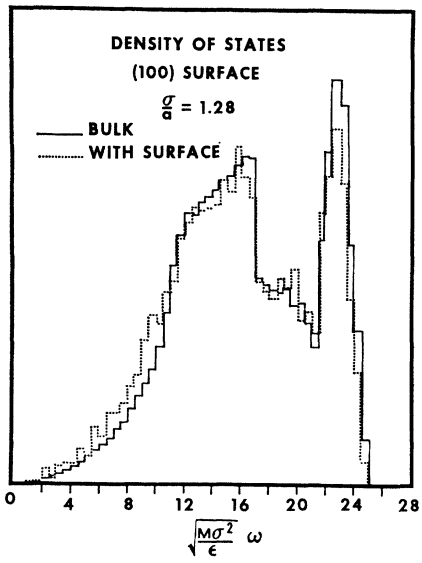

FIG. 13. Density of vibrational states at $\sigma/a=1.28$ in the bulk and for a slab-shaped crystal 21 layers thick with a (100) surface.

[21] G. K. Horton and J. W. Leech, Proc. Phys. Soc. (London) 82, 816 (1963).

[22] In calculating the dynamic displacements, one must assume a value for the density in advance. Since the assumed density (corresponding to $\sigma/a=1.28$) was not precisely correct for the temperatures at which the calculations were performed, the dynamic displacements approach asymptotic values which are not precisely zero.

In Eq. (3.9) the specific heat is expressed in terms of the vibrational frequencies. Since the summand in that equation increases monotonically as ω decreases, the specific heat is expected ordinarily to be increased by the presence of a surface. We define the surface specific heat to be the difference between the specific heat of a system of particles with a surface and the specific heat of the same number of particles in the bulk, divided by the number of surface atoms. We expect the surface specific heat to be positive, to decrease as T^2 at low temperatures, because of the two-dimensional character of a surface, and to be independent of the thickness of the crystal for sufficiently large thicknesses. For further discussion of the surface specific heat and a description of previous calculations of this quantity in various models, we refer to Ref. 6.

We have calculated the surface specific heat for the (100) surface in the following way: We assume that C_v can be broken up into a bulk contribution which is proportional to the total number of atoms NN_3 and a surface contribution which is proportional to the number of surface atoms $2N$. Calling the corresponding specific heats per particle C_v^b and C_v^s respectively, we have

$$C_v = NN_3 C_v^b + 2NC_v^s. \tag{7.1}$$

Using Eq. (7.1) and the calculated values of the specific heat for two different thicknesses N_3 and N_3', we can solve for C_v^s.

One source of difficulty in calculating the specific heat at low temperatures is the fact that only values of ω of the order of magnitude of $k_BT/\hbar$ contribute, so that if T is small it becomes necessary to include sample q points for which ω is also small—i.e., points very close to the center of the Brillouin zone. A uniform mesh of q points is thus unsatisfactory for calculating C_v. (The corresponding problem for the bulk is discussed in Ref. 23.) For this reason, successively finer meshes were used as the origin was approached. Five meshes were used altogether, giving a total of 56 independent points. As a test on the accuracy, the calculation for a thickness of 11 layers was repeated with up to eight meshes; none of the results was changed by more than 0.25%.

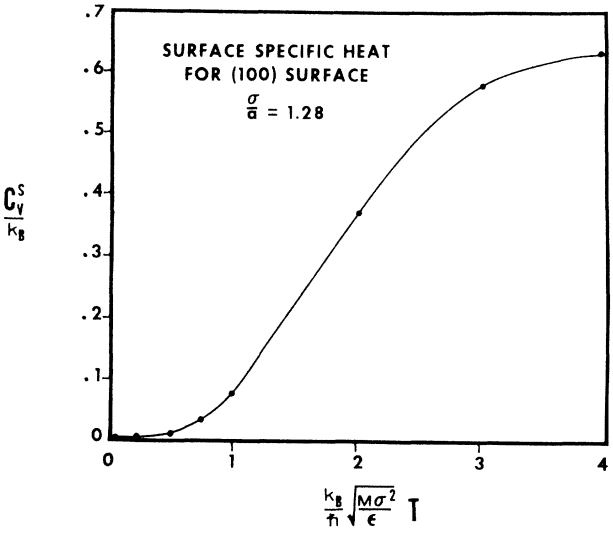

FIG. 14. Surface specific heat C_v^s for (100) surface at $\sigma/a=1.28$. The results for $N_3=11$, $N_3'=21$ and for $N_3=21$, $N_3'=31$ coincide to within the thickness of the line drawn.

In Fig. 14, the results of two calculations of the specific heat for different thicknesses are shown. In the first calculation, $N_3=11$ and $N_3'=21$; in the second, $N_3=21$ and $N_3'=31$. It can be seen that C_v^s is positive, as expected. It is also found to be almost independent of thickness and to show the expected T^2 behavior at very low temperatures.

VIII. CONCLUDING REMARKS

The object of this work has been to carry out comprehensive first-principle calculations of static and dynamic surface effects in crystals, using a realistic model which may be taken to represent the noble gas solids. In order to carry through this program, certain assumptions and approximations had to be made. In the following we shall briefly summarize these approximations and discuss the way in which they affect the results.

First of all, we have assumed that the noble-gas atoms interact through an LJ (6,12) potential. In recent years there has been increasing criticism of the LJ potential, and it is widely agreed that it is not the best potential to describe the pair interaction of noble-gas atoms. Its great virtue, however, is its analytical simplicity, and the use of any other potential would have made this work far more complicated. In addition, the LJ potential is known to give good results in calculations of both static[24] and dynamic[25] properties of noble-gas solids, the agreement with experiment often depending on the way in which the potential parameters ϵ and σ have been determined. Since all of the present calculations, except those of the dynamic displacements, have been carried out in dimensionless form, the results are independent of ϵ and σ and can thus be used with any improved set of potential parameters. We therefore view the LJ potential as a model potential, but one which is quite realistic.

The other approximations involved in our model, such as the finite thickness of the model crystal and the assumption that the displacements have their

[23] F. W. de Wette, L. H. Nosanow, and N. R. Werthamer, Phys. Rev. 162, 824 (1967).

[24] The density predicted by the LJ potential in the static approximation agrees quite well with experiment. Also, Benson and Claxton (Ref. 17) found that their results for the static displacements calculated with the LJ potential agreed rather well with the average of the results for Ne, Ar, Kr, and Xe calculated with a Buckingham potential.

[25] See, for example, F. W. de Wette and R. M. J. Cotterill, Solid State Commun. 6, 227 (1968).

static values, have been shown to be well-justified (for Ar, Kr, and Xe), provided that the temperature is not too high. It is believed, therefore, that the only important assumption in our model at low temperatures is the validity of the quasiharmonic approximation; i.e., the assumption that anharmonic effects are negligible.

At high temperatures, where the mean-square amplitudes are large, the validity of the quasiharmonic approximation is certainly open to question. This is particularly true at the surface, where the mean-square amplitudes are much larger than those in the bulk. Furthermore, we have seen in Sec. VI that the dynamic displacements are much larger than the static displacements at high temperatures, and in Sec. V we have found that the displacements have a substantial influence on the calculated quantities. Therefore, one expects both the quasiharmonic approximation and the assumption that the displacements have their static values to break down at high temperatures. In II results will be presented which were obtained by means of molecular dynamics, a method which is suitable at high temperatures and which takes both dynamic displacements and anharmonic effects into account automatically.

Most of the calculations reported here were performed for $\sigma/a=1.28$, which corresponds to the density of argon at low temperatures. Two of the calculated quantities—the displacements of the mean positions and the mean-square amplitudes—can in principle be measured by means of low-energy electron diffraction. This same technique can be used to study the thermal diffuse scattering, for which calculated results will be published elsewhere.[26] It would be extremely interesting if low-energy electron diffraction studies of noble-gas crystals could be undertaken, since such studies would provide a direct link between experiment and theory in the areas of surface structure and surface dynamics.

APPENDIX A: DEPENDENCE OF STATIC DISPLACEMENTS UPON DISTANCE FROM THE SURFACE

Consider a semi-infinite crystal which is composed of identical particles interacting through a potential $\phi(\mathbf{r}-\mathbf{r}')$ such that

$$\phi(\mathbf{r}-\mathbf{r}')\approx c|\mathbf{r}-\mathbf{r}'|^{-p} \tag{A1}$$

for large $|\mathbf{r}-\mathbf{r}'|$, where c is a constant and p is an integer >3. We show that for m sufficiently large

$$\delta_m=\text{const}\times 1/m^{p-3}. \tag{A2}$$

The structure of the crystal and the type of surface are immaterial, except that the surface is assumed to be a plane of the crystal. It is also assumed that each plane is displaced as a whole, and that the displacements are small.

The condition for static equilibrium of the crystal is

$$\frac{\partial\Phi}{\partial\delta_m}=d\sum_{\substack{\infty>n>m\\ m\geq n'\geq 1}}\sum_{\substack{l_1l_2\\ l_1'l_2'}}\frac{\partial\phi(\mathbf{r}-\mathbf{r}')}{\partial(z-z')}=0, \tag{A3}$$

where d is the distance between planes and $\mathbf{r}$ and $\mathbf{r}'$ specify positions of particles within the nth and n'th planes, respectively. If the summand on the right hand side of Eq. (A3) is expanded in a Taylor series about the bulk positions, we obtain to first order

$$\sum_{\substack{\infty>n>m\\ m\geq n'\geq 1}}\sum_{\substack{l_1l_2\\ l_1'l_2'}}\left(\frac{\partial\phi(\mathbf{r}-\mathbf{r}')}{\partial(z-z')}\right)_b + \sum_{\substack{\infty>n>m\\ m\geq n'\geq 1}}\sum_{\substack{l_1l_2\\ l_1'l_2'}}\left(\frac{\partial^2\phi(\mathbf{r}-\mathbf{r}')}{\partial(z-z')^2}\right)_b\Delta z=0. \tag{A4}$$

The subscript "b" indicates that a quantity is to be evaluated with all particles at their bulk positions, and

$$\Delta z=(z-z')-[(z-z')]_b. \tag{A5}$$

In (A4) the terms in $(\Delta z)^2$, etc. have been omitted because of our assumption that the displacements are small.

Now suppose that the semi-infinite crystal were converted into an infinite crystal by filling the space above the surface with particles. The equation for static equilibrium would then become

$$\sum_{\substack{\infty>n>m\\ m\geq n'>-\infty}}\sum_{\substack{l_1l_2\\ l_1'l_2'}}\frac{\partial\phi(\mathbf{r}-\mathbf{r}')}{\partial(z-z')}=0. \tag{A6}$$

Furthermore, since the equilibrium positions in this case would be the bulk positions, the summation in Eq. (A6) is to be evaluated with all atoms in their bulk positions. Therefore, if we break this summation up into the parts for $n'\geq 1$ and $n'\leq 0$ and make use of Eqs. (A4) and (A6), we obtain

$$\sum_{\substack{\infty>n>m\\ m\geq n'\geq 1}}\sum_{\substack{l_1l_2\\ l_1'l_2'}}\left(\frac{\partial^2\phi(\mathbf{r}-\mathbf{r}')}{\partial(z-z')^2}\right)_b\Delta z + \sum_{\substack{\infty>n>m\\ 0\geq n'>-\infty}}\sum_{\substack{l_1l_2\\ l_1'l_2'}}\left(\frac{\partial\phi(\mathbf{r}-\mathbf{r}')}{\partial(z-z')}\right)_b. \tag{A7}$$

Now we make two approximations regarding the right-hand side of this equation, both of which are valid for large $|\mathbf{r}-\mathbf{r}'|$ and hence for large m: (1) We replace $\phi(\mathbf{r}-\mathbf{r}')$ by $c|\mathbf{r}-\mathbf{r}'|^{-p}$ in accordance with Eq. (A1);

[26] F. W. de Wette and R. E. Allen, in *Proceedings of the Fourth International Symposium on The Structure and Chemistry of Solid Surfaces, Berkeley, Calif., 1968* (John Wiley & Sons, Inc., New York, 1969).

(2) We replace the sum by an integral,

$$I=-cpDN\int_m^\infty dz\int_{-\infty}^0 dz'\int_0^\infty (2\pi\rho d\rho) \times[\rho^2+(z-z')^2]^{-(p+2)/2}(z-z') \quad \text{(A8)}$$

$$=\text{const}\times 1/m^{p-3}, \quad \text{(A9)}$$

where D is the number of particles per unit volume. According to Eq. (A7), therefore,

$$\sum_{\substack{\infty>n>m\\ m\geq n'\geq 1}}\sum_{\substack{l_1l_2\\ l_1'l_2'}}\left(\frac{\partial^2\phi(\mathbf{r}-\mathbf{r}')}{\partial(z-z')^2}\right)_b\Delta z=\text{const}\times\frac{1}{m^{p-3}}. \quad \text{(A10)}$$

Suppose that the displacements can be taken to vary independently, so that all displacements except the one under consideration may be set equal to zero. Then $\Delta z=\delta_m$ for all the terms of the sum in Eq. (A10), and Eq. (A2) follows immediately.

It is not necessarily true, however, that the displacements vary independently. For example, in the case of an LJ potential the derivative in Eq. (A10) is large for nearest neighbors. When the surface is a (110) plane, there are nearest neighbors in the planes which are adjacent to a given plane and in the next planes also. Consequently, three terms in the sum of Eq. (A10) are important, and these terms contain δ_m, $(\delta_m+\delta_{m+1})$, and $(\delta_m+\delta_{m-1})$, respectively. Each displacement is thus coupled to the two adjacent to it.

In the case that the displacements do not vary independently, we make two additional assumptions: First, we assume that each displacement is coupled to only a finite number of others, so that there is some n_0 such that only δ_{m+n_0}, $\delta_{m+n_0-1},\cdots,\delta_{m-n_0}$ occur in Eq. (A10) (for $m>n_0$). Second, we assume that the solution for δ_m has the form

$$\delta_m=a_0+a_1m+\cdots+a_sm^s+a_{-1}m^{-1}+a_{-2}m^{-2}+\cdots, \quad \text{(A11)}$$

where s is an arbitrarily large positive integer. When Δz is written in terms of the displacements $\delta_{m'}$ between the nth and n'th planes, when these $\delta_{m'}$ are expressed in terms of the series in Eq. (A11), and when the binomial theorem is used to evaluate $m'^k=(m+\text{integer})^k$, then an equation of the following form results:

$$\sum_{k=0}^{s}(a_sc_{sk}+a_{s-1}c_{s-1,k}+\cdots+a_kc_{kk})m^k+\sum_{k=-\infty}^{-1}(a_{-1}c_{-1,k}+a_{-2}c_{-2,k}+\cdots+a_kc_{kk})m^k=\text{const}\times m^{-p+3}. \quad \text{(A12)}$$

The c_{ij} are constants. In order to use the binomial theorem for negative powers of m' we have assumed that $m>n_0$. If Eq. (A12) is to hold for all positive integers m, the coefficient of each m^k must vanish. Therefore $a_s=a_{-1}=0$, and by induction $a_k=0$ for $k>-p+3$. Hence, Eq. (A11) reduces to

$$\delta_m=\frac{a_{-p+3}}{m^{p-3}}+\frac{a_{-p+2}}{m^{p-2}}+\frac{a_{-p+1}}{m^{p-1}}+\frac{a_{-p}}{m^p}+\cdots \quad \text{(A13)}$$

and in the limit $m\to\infty$, Eq. (A13) in turn reduces to Eq. (A2).

Equation (A2) for uncoupled displacements and Eq. (A13) for coupled displacements were derived with no approximations except the two immediately preceding Eq. (A8) (plus the assumption that $m>n_0$). For an LJ potential, both approximations should be good for quite small values of m. We can therefore expect the inverse cube behavior to show up for small m when there is no coupling of displacements [(100) and (111) surfaces], but when there is coupling [(110) surface] the higher order terms in Eq. (A13) may persist until m is fairly large. Both these expectations are confirmed by the calculated results.

APPENDIX B: EXPRESSIONS FOR DYNAMICAL QUANTITIES IN THE CASE OF A LENNARD-JONES POTENTIAL

In this Appendix we give explicit expressions for the dynamical matrix and the physical quantities $\langle u^2\rangle$, $\langle p^2\rangle$, F, and C_v in the case of a Lennard-Jones potential. The dynamical matrix is given by

$$D_{\alpha\beta}(l_3l_{3'})=\frac{\epsilon}{M\sigma^2}\left[\left(\frac{\sigma}{a}\right)^{14}\mathrm{S}_{14}+\left(\frac{\sigma}{a}\right)^{8}\mathrm{S}_8\right], \quad \text{(B1)}$$

where

$$\mathrm{S}_{14}=-48\sum_i\left(\frac{a}{r_0^{ll'}}\right)^{14}\left[14\frac{S_{\alpha\beta}(q)}{(r_0^{ll'})^2}-\delta_{\alpha\beta}S(q)\right], \quad \text{(B2)}$$

and

$$\mathrm{S}_8=24\sum_i\left(\frac{a}{r_0^{ll'}}\right)^{8}\left[8\frac{S_{\alpha\beta}(q)}{(r_0^{ll'})^2}-\delta_{\alpha\beta}S(q)\right] \quad \text{(B3)}$$

with

$$S_{\alpha\beta}(q)=\sum_j\alpha_0^{ll'}\beta_0^{ll'}\exp[iq\cdot(r_0^{l}-r_0^{l'})] \quad \text{(B4)}$$

and

$$S(q)=\sum_j\exp[iq\cdot(r_0^{l}-r_0^{l'})]. \quad \text{(B5)}$$

Here i labels a shell of atoms with the same distance from the origin and j labels the atoms within a shell, so that summing over i and j is equivalent to summing over l_1' and l_2'. If $l_3'=l_3$, then the $l_1'=l_2'=0$ terms in Eqs. (B2) and (B3) are, respectively, to be replaced by

$$48\sum_{l_3''}\sum_i{}'\left(\frac{a}{r_0^{ll''}}\right)^{14}\left[14\frac{S_{\alpha\beta}(q=0)}{(r_0^{ll''})^2}-\delta_{\alpha\beta}S(q=0)\right], \quad \text{(B6)}$$

and

$$-24\sum_{l_3''}\sum_i{}'\left(\frac{a}{r_0^{ll''}}\right)^{8}\left[8\frac{S_{\alpha\beta}(q=0)}{(r_0^{ll''})^2}-\delta_{\alpha\beta}S(q=0)\right], \quad \text{(B7)}$$

where the prime indicates that the point $l_1''=l_2''=0$ is to be omitted if $l_3''=l_3$.

For an LJ potential, we can define the dimensionless quantities

$$\Omega_p(q)=(M\sigma^2/\epsilon)^{1/2}\omega_p(q), \tag{B8}$$

$$T^*=(k_B/\hbar)(M\sigma^2/\epsilon)^{1/2}T, \tag{B9}$$

$$x=\Omega_p(q)/T^*. \tag{B10}$$

In terms of these quantities, Eqs. (3.6)–(3.9) can be rewritten as follows:

$$\frac{(M\epsilon)^{1/2}}{\hbar\sigma}\langle u_\alpha^2(l_3)\rangle=\frac{1}{2N}\sum_{qp}{}'\frac{|\xi_\alpha(l_3;qp)|^2}{\Omega_p(q)}\frac{e^x+1}{e^x-1}, \tag{B11}$$

$$\frac{\sigma}{\hbar(M\epsilon)^{1/2}}\langle p_\alpha^2(l_3)\rangle=\frac{1}{2N}\sum_{qp}{}'|\xi_\alpha(l_3;qp)|^2\Omega_p(q)\frac{e^x+1}{e^x-1}, \tag{B12}$$

$$\frac{1}{\hbar}\left(\frac{M\sigma^2}{\epsilon}\right)^{1/2}F=\sum_{qp}{}'\left[\frac{\Omega_p(q)}{2}+T^*\ln(1-e^{-x})\right], \tag{B13}$$

$$\frac{1}{k_B}C_v=\sum_{qp}{}'\frac{x^2e^x}{(e^x-1)^2}. \tag{B14}$$

The summations over q in Eqs. (B11)–(B14) in principle extend over the complete two-dimensional Brillouin zone. In practice, however, it is sufficient to use only the irreducible element, which comprises $\frac{1}{8}$, $\frac{1}{12}$, and $\frac{1}{4}$ the full zone for the (100), (111), and (110) surfaces, respectively (see Fig. 3). If $w(q)$ is the number of points in the full zone represented by the point q in the irreducible element, then the summations need only extend over the irreducible element provided that each term is multiplied by $w(q)$. There is one exception: For the (100) and (111) surfaces the prescription for $\alpha=x$ or y is

$$|\xi_\alpha(l_3)|^2\rightarrow\tfrac{1}{2}w(q)[|\xi_x(l_3)|^2+|\xi_y(l_3)|^2]. \tag{B15}$$

APPENDIX C: REDUCTION OF THE DYNAMICAL MATRIX

In this Appendix we show that the original dynamical matrix for a slab-shaped crystal can always be reduced to a real, symmetric matrix of the same size. Use of this reduced matrix results in a very great saving in the computer time required to calculate the eigensystem.

The method for reducing the dynamical matrix does not depend upon the crystal structure, the interaction between particles, or the type of surface. It is assumed only that the slab possesses a center of inversion and has a structure which is periodic with respect to some set of translations parallel to the surface; i.e., we assume that the same two-dimensional Bravais lattice can be used to describe all the planes, but that the unit cell associated with a lattice point may differ from one plane to another in the number and kind of particles it contains and in their positions. The particles in a unit cell of the l_3th plane are labeled by $\kappa=1,2,\cdots,s(l_3)$. Equations (3.1)–(3.9) still hold, with the quantities now depending on κ and with Φ now signifying the total static energy due to any kind of interaction. From Eq. (3.4) it follows that

$$\Phi_{\beta\alpha}(\mathbf{l}'\kappa';\mathbf{l}\kappa)=\Phi_{\alpha\beta}(\mathbf{l}\kappa;\mathbf{l}'\kappa') \tag{C1}$$

and from Eq. (3.3)

$$D_{\beta\alpha}(l_3'\kappa';l_3\kappa)=\frac{1}{[M_{\kappa'}(l_3')M_\kappa(l_3)]^{1/2}}\times\sum_l\Phi_{\beta\alpha}(\mathbf{l}'\kappa';\mathbf{l}\kappa)e^{iq\cdot(r_0l'-r_0l)}. \tag{C2}$$

It makes no difference whether we sum over l or over l' in Eq. (C2). Equations (C1) and (C2) therefore imply that

$$D_{\beta\alpha}(l_3'\kappa';l_3\kappa)=\frac{1}{(M_\kappa(l_3)M_{\kappa'}(l_3'))^{1/2}}\times\sum_{l'}\Phi_{\alpha\beta}(\mathbf{l}\kappa;\mathbf{l}_3'\kappa')e^{-iq\cdot(r_0l-r_0l')} \tag{C3}$$

$$=D_{\alpha\beta}{}^*(l_3\kappa;l_3'\kappa'). \tag{C4}$$

Hence the dynamical matrix is Hermitian.

Now we take the origin ($\mathbf{r}_0{}^l=\mathbf{l}=0$) to lie at the crystal's center of inversion, so that the force constants are invariant under the transformation $\mathbf{l}\rightarrow-\mathbf{l}$:

$$\Phi_{\alpha\beta}(-\mathbf{l}\kappa;-\mathbf{l}'\kappa')=\Phi_{\alpha\beta}(\mathbf{l}\kappa;\mathbf{l}'\kappa') \tag{C5}$$

(κ is chosen such that the unit cell is reversed for $l_3<0$.) By definition,

$$D_{\alpha\beta}(-l_3\kappa;-l_3'\kappa')=\frac{1}{[M_\kappa(-l_3)M_{\kappa'}(-l_3')]^{1/2}}\times\sum_{-l'}\Phi_{\alpha\beta}(-\mathbf{l}\kappa;-\mathbf{l}'\kappa')e^{iq\cdot(r_0-l-r_0-l')}, \tag{C6}$$

where l' has been renamed $-l'$. Since $M_\kappa(-l_3)=M_\kappa(l_3)$, $\mathbf{r}_0{}^{-l}=-\mathbf{r}_0{}^l$, and summing over $-l'$ is equivalent to summing over l', Eqs. (C5) and (C6) imply that

$$D_{\alpha\beta}(-l_3\kappa;-l_3'\kappa')=D_{\alpha\beta}{}^*(l_3\kappa;l_3'\kappa'). \tag{C7}$$

Because the dynamical matrix is Hermitian, ω^2 is real, so Eqs. (C7) and (3.2) imply that we can take

$$\xi_\alpha(-l_3\kappa)=\xi_\alpha{}^*(l_3\kappa). \tag{C8}$$

Next we define the matrix

$$
\begin{aligned}
W_{\alpha\beta}(l_3\kappa;l_3'\kappa') &= \mathrm{Re}D_{\alpha\beta}(l_3\kappa;l_3'\kappa')+\mathrm{Re}D_{\alpha\beta}(l_3\kappa;-l_3'\kappa'), \\
&\qquad\qquad l_3>0,\ l_3'>0 \\
&= \mathrm{Im}D_{\alpha\beta}(l_3\kappa;l_3'\kappa')-\mathrm{Im}D_{\alpha\beta}(l_3\kappa;-l_3'\kappa'), \\
&\qquad\qquad l_3>0,\ l_3'<0 \\
&= -\mathrm{Im}D_{\alpha\beta}(l_3\kappa;l_3'\kappa')-\mathrm{Im}D_{\alpha\beta}(l_3\kappa;-l_3'\kappa'), \\
&\qquad\qquad l_3<0,\ l_3'>0 \\
&= \mathrm{Re}D_{\alpha\beta}(l_3\kappa;l_3'\kappa')-\mathrm{Re}D_{\alpha\beta}(l_3\kappa;-l_3'\kappa'), \\
&\qquad\qquad l_3<0,\ l_3'<0 \\
&= \sqrt{2}\ \mathrm{Re}D_{\alpha\beta}(l_3\kappa;0\kappa'),\quad l_3>0,\ l_3'=0 \qquad \text{(C9)} \\
&= -\sqrt{2}\ \mathrm{Im}D_{\alpha\beta}(l_3\kappa;0\kappa'), \\
&\qquad\qquad l_3<0,\ l_3'=0 \\
&= \sqrt{2}\ \mathrm{Re}D_{\alpha\beta}(0\kappa;l_3'\kappa'),\quad l_3=0,\ l_3'>0 \\
&= \sqrt{2}\ \mathrm{Im}D_{\alpha\beta}(0\kappa;l_3'\kappa'),\quad l_3=0,\ l_3'<0 \\
&= \mathrm{Re}D_{\alpha\beta}(0\kappa;0\kappa'),\quad l_3=0,\ l_3'=0
\end{aligned}
$$

and the vector

$$
\begin{aligned}
v_\alpha(l_3\kappa) &= \sqrt{2}\ \mathrm{Re}\xi_\alpha(l_3\kappa), \quad l_3>0 \\
&= \mathrm{Re}\xi_\alpha(0\kappa), \quad l_3=0 \qquad \text{(C10)} \\
&= \sqrt{2}\ \mathrm{Im}\xi_\alpha(-l_3\kappa) \quad l_3<0.
\end{aligned}
$$

Since the $\xi_\alpha(l_3\kappa)$ are orthonormal, so are the $v_\alpha(l_3\kappa)$. Eqs. (C4) and (C7) imply that

$$
W_{\beta\alpha}(l_3'\kappa';l_3\kappa)=W_{\alpha\beta}(l_3\kappa;l_3'\kappa'). \qquad \text{(C11)}
$$

Finally, by substitution and use of Eqs. (C7), (C8), and (3.2), one can show that

$$
\sum_{\beta l_3'\kappa'} W_{\alpha\beta}(l_3\kappa;l_3'\kappa')v_\beta(l_3'\kappa')=\omega^2 v_\alpha(l_3\kappa). \qquad \text{(C12)}
$$

The eigensystem of $D_{\alpha\beta}(l_3\kappa;l_3'\kappa')$ can thus be obtained from that of $W_{\alpha\beta}(l_3\kappa;l_3'\kappa')$ in a very simple way: The eigenvalues are the same and

$$
\xi_\alpha(l_3\kappa)=\tfrac{1}{2}\sqrt{2}[v_\alpha(l_3\kappa)+iv_\alpha(-l_3\kappa)]. \qquad \text{(C13)}
$$

It should be mentioned here that Wallis, Clark, and Herman[8] have previously shown how the dynamical matrix for their model can be reduced.

APPENDIX D: DIVERGENCE OF THE MEAN-SQUARE AMPLITUDES IN INFINITE SLAB-SHAPED CRYSTALS

It is well-known that the mean-square amplitudes of vibration for a two-dimensional crystal diverge logarithmically at finite temperatures as the size of the crystal increases (see, for example, Ref. 18, pp. 241–242). The same is true for slab-shaped crystals, as can be seen from Eq. (3.6): The sum over p in this equation involves $3N_3-3$ "optical" modes, for which ω_p approaches a fixed value as $|q|\to 0$, and 3 "acoustic" modes, for which $\omega_p \propto |q|$ for small $|q|$. Therefore, when $|q|$ is sufficiently small, the contribution from the acoustic modes dominates the summand in Eq. (3.6) and the summand is proportional to $1/|q|^2$ for $T\neq 0$. The contribution from a small circle of radius q_0 about the origin in reciprocal space is then roughly proportional to

$$
\lim_{\delta\to 0}\int_\delta^{q_0}\frac{2\pi|q|d|q|}{|q|^2}=2\pi\lim_{\delta\to 0}\ln(q_0/\delta) \qquad \text{(D1)}
$$

which diverges.

As long as the number of atoms per plane, and thus the periodicity lengths in the x and y directions, are finite the smallest allowed values of q in the first Brillouin zone are a finite distance away from the origin, and hence the mean-square amplitudes are finite. However, for small thicknesses one can observe an increase in the mean-square amplitudes at high temperatures as the periodicity length is increased. For example, in Table II it can be seen that when the number of sample points was increased from 9 to 64, the mean-square amplitudes at both the surface and the center of the slab-shaped crystal increased by several percent. At $T=0$°K, where there is no divergence problem, the change was only a fraction of one percent.

As the thickness of the crystal is increased, the value of $|\xi_\alpha(l_3;qp)|^2$ for a given mode decreases because of the normalization condition on the eigenvectors. Consequently, the contribution of the acoustic modes to the mean-square amplitudes is roughly proportional to $1/N_3$; i.e., the divergence of the mean-square amplitudes with respect to increasing periodicity length (and hence the effect of changes in the number of sample points) decreases in inverse proportion to the thickness of the crystal. As $N_3\to\infty$, the divergence disappears entirely.

In order to obtain very accurate results for slab-shaped crystals at high temperatures, one would have to use model crystals of very great thickness. Even in the high-temperature regime, however, if the periodicity length is approximately equal to the thickness, the error for a crystal of moderate thickness (about 20 layers) should be only a few percent. It can be seen in Table II that the results for a crystal with a thickness of 21 layers, with 30 points in the irreducible element, agree with the result of an independent calculation for the bulk to within about 1%. The error decreases with temperature, and at absolute zero there is agreement to four significant figures.